High-speed Railway 1 (2023) 171–178

Contents lists available at ScienceDirect

High-speed Railway

journal homepage: www.keaipublishing.com/en/journals/high-speed-railway

Research article

Refined disturbance observer based prescribed performance fixed-time control of high-speed EMS trains with track irregularities

Yiran Xie, Boyang Zhao, Xiuming Yao*

School of Electronics and Information Engineering, Beijing Jiaotong University, Beijing 100044, China

ARTICLE INFO

Keywords:
High-speed electromagnetic suspension train
Track irregularity
Refined disturbance observer
Prescribed performance
Fixed-time control

ABSTRACT

High-speed Electromagnetic Suspension (EMS) train is continuously impacted by the irregularity of the track, which worsens the levitation performance of the train. In this paper, a composite control scheme for the EMS is proposed to suppress track irregularities by integrating a Refined Disturbance Observer (RDO) and a Prescribed Performance Fixed-Time Controller (PPFTC). The RDO is designed to estimate precisely the track irregularities and lumped disturbances with uncertainties and exogenous disturbances in the suspension system, and reduce input chattering by applying to the disturbance compensation channel. PPFTC is designed to converge the suspension air gap error to equilibrium point with prescribed performance by completing error conversion, and solve the fast dynamic issue of EMS. And the boundary of overshoot and steady-state is limited in the ranged prescribed. A theoretical analysis is conducted on the stability of the proposed control method. Finally, the effectiveness and reasonability of the proposed composite anti-disturbance control scheme is verified by simulation results.

1. Introduction

High-speed Electromagnetic Suspension (EMS) train achieves non-contact suspension and guidance between the train and the track by electromagnetic force [1]. The main key to the successful implementation of EMS lies in the extensive research and application of suspension systems. The EMS is a strongly nonlinear system. Proportional-Integral-Differential (PID) and Proportional-Differential (PD) controllers are usually proposed to effectively control system by adjusting the gain parameters [2]. But these controllers cannot be used in more complex industrial scenarios. An adaptive fixed-time control algorithm is used to ensure the steady-state performance of the suspension system by converging within a fixed time [3]. Nonsingular terminal sliding mode control based on adaptive laws can ensure the dynamic and steady-state performance of the system by allowing the switching gain in sliding mode dynamics to be adaptively adjusted according to the system state [4].

The track may be irregular for some reasons such as material production, line installation, external environment and so on [5]. Track irregularities can affect the stability of the suspension system and reduce passenger comfort [6]. Furthermore, many researchers have done a lot of work on track irregularities [7,8]. The finite element method is used to establish the train-track nonlinear coupled system, which can improve the analysis efficiency of the nonlinear coupling system [9]. However, the persistent excitation of track irregularities for train brings a huge challenge that achieving fast convergence, high accuracy estimation and robustness of the suspension system.

Sliding Mode Control (SMC) technology is used widely in uncertain nonlinear systems. For instance, unmanned aerial vehicle [10], robotic manipulators [11] and so on. However, the problem of system oscillation caused by the existence of discontinuous high-frequency components cannot be ignored. Some methods have been proposed to avoid this phenomenon. The design of boundary layer can effectively avoid or weaken buffeting [12]. Additionally, too large or too small boundary layer will cause a negative effect of the controller. The use of high-order SMC technology can effectively solve chattering while ensuring system robustness but it is mathematically intensive [13]. Terminal SMC (TSMC) [14], fast TSMC [15], non-singular TSMC [16], and non-singular fast TSMC [17] have been proposed to overcome the shortcomings of SMC, and have advantages such as robustness to uncertainties and finite time convergence and so on. However, these methods will also produce inevitably buffeting.

Fortunately, the disturbance compensation technology can also effectively reduce SMC chattering phenomenon. The Disturbance Observer (DO) is introduced to estimate uncertain components and

* Corresponding author.
E-mail address: xmyao@bjtu.edu.cn (X. Yao).

https://doi.org/10.1016/j.hspr.2023.09.001
Received 2 August 2023; Received in revised form 10 August 2023; Accepted 16 August 2023
Available online 5 September 2023

compensate the disturbance estimation for the controller. In addition, the track irregularities in the suspension system are also compensated as mismatched disturbances by using Disturbance Observer-Based Control (DOBC) [18]. The Extended State Observer (ESO) has a good estimation effect on the lumped disturbances composed of modeling dynamics, uncertainty and external disturbances [19]. In Ref. [20], constant value disturbance and harmonic disturbance are described as exogenous system for designing DOs to suppress and eliminate disturbances. In Ref. [21], the high-order DO is designed for accurate estimation of uncertain harmonic disturbance. For systems with multiple disturbances, the H_∞ theory can be used to construct a hierarchical control algorithm that conforms to the hierarchy [22,23]. Some improved higher-order DOs can achieve finite time convergence to accelerate system response [24,25].

In recent years, composite anti-disturbance controllers have been applied in the research of the suspension system. In Ref. [26], a new control strategy is proposed to solve the issue of fast dynamics of the suspension system for the high-speed EMS train with track irregularities. The suspension system considers a semi bogie and the designed fixed-time synchronization controller has satisfactory control performance [27]. The composite control strategy of adaptive terminal SMC combined with ESO reduces the chattering and it is globally uniformly bounded stable [28]. Ref. [29] proposed a terminal SMC which can improve the rate of convergence of the system in a finite time. In suspension system affected by uncertainties and exogenous disturbances, the integration SMC and ESO are combined to improve the rate of convergence and have better steady-state performance in the system [30].

Tracking the reference trajectory of the suspension air gap in the suspension system under track irregularities is a highly challenging task. Therefore, this paper focuses on the tracking problem of the suspension air gap in the suspension system under track irregularities and lumped disturbances with uncertainties and external disturbances. As shown in Fig. 1, the Refined Disturbance Observer based Prescribed Performance Fixed-Time Control (RDO-PPFTC) strategy is proposed. The main contributions of this paper are as follows,

1) Considering the impact of track irregularity, an improved dynamic model of high-speed electromagnetic suspension train is proposed. In actual operation, track irregularity continuously excites the suspension system. This issue needs to be considered in the suspension system.
2) Prescribed Performance Function (PPF) is introduced to convert steady-state errors and ensure that the tracking error can converge to zero when the conversion error converges to zero. At the same time, the relevant performance of the controller is dynamically constrained in a given functional domain and the control performance is improved.
3) RDO integrates the advantages of DO and ESO to achieve high-precision estimation of track irregularities. The PPFTC designed based on RDO can achieve the limitation of error performance upper and lower boundaries and ensure the suspension system can converge within a prescribed time and have good effects in tracking accuracy, fast convergence, stability, and reducing chattering.

The remaining parts of this paper are as follows. Section 2 provides a problem statement and constructs the suspension system model. Section 3 introduces the design process of the proposed the refined disturbance observer based prescribed performance fixed-time control. The effectiveness of the proposed control scheme was verified by simulation results in Section 4. Finally, Section 5 gives a conclusion.

2. Problem statement

The track irregularities and lumped disturbances with uncertainties and external disturbances will have adverse effects on train operation. Therefore, these two types of disturbances need to be considered when establishing the suspension system model. The simplified model of the suspension system considering a single electromagnet is shown in Fig. 2, where $w_0(t)$ represents the position of the absolute track reference plane. The actual suspension air gap is

$$x(t) = w_2(t) - w_1(t) \tag{1}$$

where $w_1(t)$ is the actual track height, and $w_2(t)$ is the position of the suspension electromagnet.

The dynamic equation of the suspension system can be determined by Newton's second law

$$m\frac{\mathrm{d}^2 w_2(t)}{\mathrm{d}t^2} = mg - F(t) - F_\mathrm{e}(t) \tag{2}$$

where m and g are the mass of suspension electromagnet and gravitational acceleration respectively. $F(t)$is the electromagnetic levitation force which can be expressed as

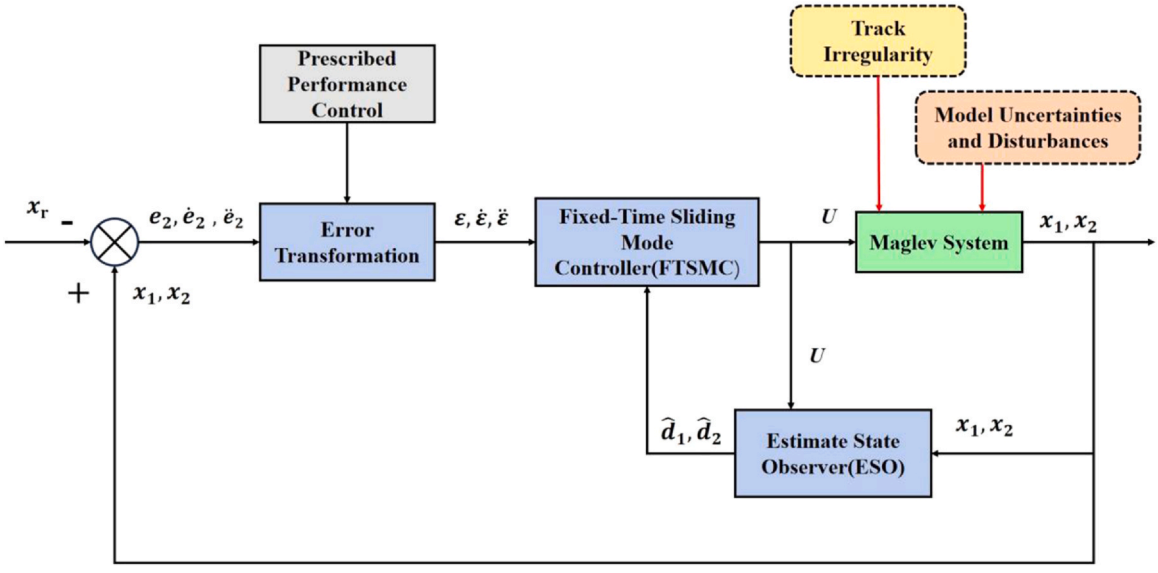

Fig. 1. Block diagram of proposed control strategy.

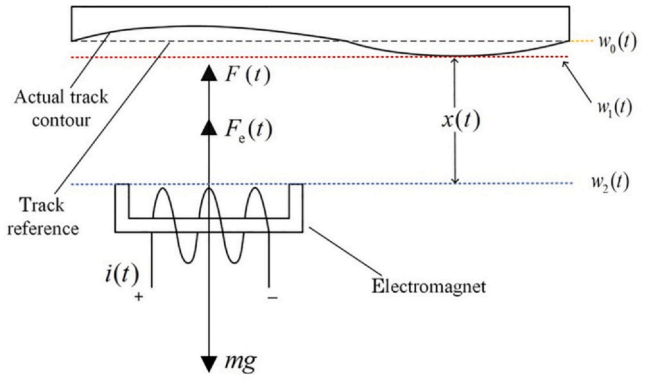

Fig. 2. A simplified diagram of suspension system considering track irregularities and external disturbance.

$$F(t) = \frac{\mu_0 N^2 S}{4m}\frac{i^2(t)}{x^2(t)} \tag{3}$$

where μ_0, S, N denote the Vacuum permeability, the positive cross-sectional area, the number of turns of electromagnetic coil, respectively; $F_e(t)$ is an external disturbance. For the convenience of subsequent calculations, Eq. (2) is rewritten as follows

$$m\ddot{w}_2 = mg - hu - F_e \tag{4}$$

where $h = \frac{\mu_0 N^2 S}{4x^2}$ is a parameter of suspension force, $u = i^2$ is the control effort.

Due to the uncertainty parameters h and external disturbance F_e in the suspension system, considering the parameter changes, uncertainties caused by external disturbance, the overall suspension system can be rewritten as

$$m\ddot{w}_2 = mg - (h + \Delta h)u - F_e \tag{5}$$

where $\Delta h \in \mathbb{R}$ represents the parameter uncertainty of the system.

By differentiating Eq. (1) and combining Eqs. (4) and (5), the suspension system can be redefined as

$$\begin{cases} \dot{x}_1 = x_2 + d_1, \\ \dot{x}_2 = g - Hu + d_2 \end{cases} \tag{6}$$

where x_1 is the actual suspension air gap, $x_2 = \dot{w}_2$ is the vertical velocity of suspension system, $H = \frac{h}{m}$, and d_2 is the lumped disturbance of uncertainty and external disturbance, which is described as

$$d_2 = \frac{1}{m}(-\Delta h u - F_e) \tag{7}$$

In addition, $d_1 = \dot{w}_1$ is the track irregularity disturbance which can be described by the following exogenous models [20]

$$\begin{cases} \dot{\xi} = \boldsymbol{W}\xi \\ d_1 = \boldsymbol{V}\xi \end{cases} \tag{8}$$

where $\xi \in \mathbb{R}^2$ is the auxiliary state of model (8), $\boldsymbol{W} \in \mathbb{R}^{2\times 2}$ and $\boldsymbol{V} \in \mathbb{R}^{1\times 2}$ are known coefficient matrices.

Remark 1. The EMS increases the frequency of irregularity signals [26]. Therefore, d_1 which introduces rapid dynamics into magnetic suspension devices has caused obstacles to the stability of the suspension system and the design of the controller.

Remark 2. When a high-speed EMS train runs to the track section with ramp, the gravitational acceleration direction is shifted, resulting in the gravitational acceleration being only the cosine value on the plane track [31]. The missing gravitational acceleration at this time is summed up as the lumped disturbance d_2.

Before designing the controller, we propose some assumptions as follow.

Assumption 1. Track irregularity disturbance has a first derivative, resulting in $|w_1(t)| < \dot{w}_1$ and $|\dot{w}_1(t)| \leqslant \dot{\bar{w}}_1$ established, where $\bar{w}_1$ and $\dot{\bar{w}}_1$ are the supremum of w_1 and $\dot{w}_1$, respectively.

Remark 3. In actual track design, the amplitude of track width must meet the requirements of line design and the amplitude of track irregularity is limited, so w_1 is bounded. At the same time, trains must use magnets with limited area to pass through the track and the rate of change in track position must also be bounded, so the first derivative of w_1 can be considered bounded.

Assumption 2. The lumped disturbance $d_1$has a supremum, i.e., $0 < |d_2| \leqslant \bar{d}_2$, where $\bar{d}_2$ is the supremum of d_2.

Remark 4. Due to the influence of machining errors in the actual track design process, even when meeting the line design standards, there may be slight parameter disturbances in the system; The external disturbances force that affect the electromagnetic levitation train in operation mainly include the coupling force, secondary suspension force, and aerodynamic lift force. Therefore, d_2 is bounded.

Next, the necessary definitions and theorems for the control strategy will be proved.

Definition 1. (*fixed–time stability*) [32] Consider a continuous system

$$\dot{z}(t) = f(z(t)), f(0) = 0, z(t) \in \mathbb{R}^n \tag{9}$$

where $f(\cdot)$: $\mathbb{R}^n \to \mathbb{R}^n$is a continuous function, $z(t)$ continuous represent the system state, $\dot{z}(t)$ is the derivative of $z(t)$ with respect to time. If there exist positive real numbers $T(z)$ and $\alpha(\alpha \leqslant 1)$ such that for any initial state $z(a) \in \mathbb{R}^n$, the system state satisfies the inequality $\|z(t) - z(a)\| \leqslant \alpha$, $\forall\, t \geqslant T(z)$ after a time $t = T(z)$. Then the system (9) achieves stability within the fixed time $T(z)$.

Lemma 1. [33] for the system (9), if there is a positive definite function $V_0(x)$ and it satisfies

$$\dot{V}_0(x) \leqslant -aV^{\frac{m}{n}}(x) - cV^{\frac{p}{q}}(x) \tag{10}$$

where a, $c > 0$, m, n, p, q are positive odd integers that satisfy $m > n$, $p < q$, the system states will converge to the origin in fixed-time given by

$$T \leqslant \frac{1}{a}\cdot\frac{n}{m-n} + \frac{1}{c}\cdot\frac{q}{q-p} \tag{11}$$

The suspension system is an unstable and highly nonlinear system. It is a huge challenge to track the trajectory of suspension air gap. Hence, this paper proposes a new control strategy that considers the condition that track irregularities and lumped disturbances with uncertainties and external disturbance and ensures that the suspension air gap can reach and stabilize at the prescribed position within a fixed-time and perform different track tracking tasks.

3. Design of the RDO-PPFTC

In this section, RDO is designed to estimate disturbances d_1 and d_2. The prescribed performance method performs error conversion and performance limitation on state errors. Then, fixed-time feedback compensation is applied to design PPFTC control law. It ensures high accuracy tracking control of the suspension air gap in the suspension

system under track irregularities and lumped disturbances with uncertainly and exogenous disturbance.

3.1. Design of Refined Disturbance Observer (RDO)

Due to the presence of unmatched disturbance d_1 and matched disturbance d_2 in system (6), RDO is designed as an integration of DO and ESO, estimating disturbance d_1 and d_2 respectively, and then sending the estimated disturbance values as output feedforward compensation to the controller to suppress and attenuate most of the disturbance.

The DO for d_1 is presented as follows

$$\begin{cases} \hat{d}_1 = V\hat{\xi} \\ \dot{\hat{\xi}} = \upsilon + Lx_1 \\ \dot{\upsilon} = (W - LV)\hat{\xi} - Lx_2 \end{cases} \tag{12}$$

where $\hat{\xi}$ and $\hat{d}_1$ are the estimates of ξ and d_1, respectively. L is the observer gain to be designed, and υ is auxiliary variable.

Additionally, use the following ESO to estimate augmented state d_2

$$\begin{cases} \dot{\hat{x}}_2 = g - Hu + \hat{d}_2 + \eta_1\tilde{x}_2 \\ \dot{\hat{d}}_2 = \eta_2\tilde{x}_2 \end{cases} \tag{13}$$

where $\tilde{x}_2 = x_2 - \hat{x}_2$ is the observation error value of x_2. $\hat{x}_2$ and $\hat{d}_2$ are the estimates of vertical velocity x_2 and lumped disturbance d_2, respectively. These variables $\eta_1 > 0$ and $\eta_2 > 0$ are the gains of ESO to be determined.

In the following Sections, $\hat{d}_1$ and $\hat{d}_2$ will be used to design the control law.

3.2. Selection of observer gains

Based on (8) and (12), the dynamics estimation error is described as

$$\dot{\tilde{\xi}} = (W - LV)\tilde{\xi} \tag{14}$$

where $\tilde{\xi} = \xi - \hat{\xi}$ is the estimate error of the DO (12).

Similarly, based on (6) and (13), the dynamics of the estimation error can be described as follows

$$\begin{cases} \dot{\tilde{x}}_2 = \tilde{d}_2 - \eta_1\tilde{x}_2 \\ \dot{\tilde{d}}_2 = -\eta_2\tilde{x}_2 \end{cases} \tag{15}$$

where $\tilde{x}_2 = x_2 - \hat{x}_2$ and $\tilde{d}_2 = d_2 - \hat{d}_2$ denote the estimates errors of ESO.

Rewrite Eq. (15) as follows

$$\begin{bmatrix} \dot{\tilde{x}}_2 \\ \dot{\tilde{d}}_2 \end{bmatrix} = \begin{bmatrix} -\eta_1 & 1 \\ -\eta_2 & 0 \end{bmatrix} \begin{bmatrix} \tilde{x}_2 \\ \tilde{d}_2 \end{bmatrix} \tag{16}$$

Then, according to the pole assignment principle [34], the observer gains of RDO are selected as

$$|sI - (W - LV)| = (s + \omega_{0k}) \tag{17}$$

$$\left| sI - \begin{bmatrix} -\eta_1 & 1 \\ -\eta_2 & 0 \end{bmatrix} \right| = \prod_{p=1}^{r_1+1} (s + \omega_{1p}) \tag{18}$$

where ω_{0k} and ω_{1p} are positive constants. Then, system (14) and (15) are asymptotically stable and Bounded-Input Bounded-Output (BIBO) stable, respectively [35].

Remark 5. It can be seen from Section 2 that it is difficult to achieve the suspension air gap tracking control the task of the suspension system because of the existence of unmatched disturbance d_1 and the lumped disturbance d_2. In this paper, the RDO in (12) and (13) integrates DO and ESO is designed to estimate different types of disturbances, and the gains are determined by pole assignment method. Compared with the single ESO, this treatment can fully utilize prior known disturbance information and improve disturbance estimation performance.

3.3. Error transformation based on prescribed performance function

In this section, a prescribed performance function is introduced to convert the tracking error for the goal of improving the stability and convergence accuracy of the suspension system. Defining tracking error of suspension air gap x_1 as $e_1 = x_1 - x_r$, x_r is the reference suspension air gap value. Selecting the following error performance indicator function

$$\vartheta(t) = (\vartheta_0 - \vartheta_\infty)\mathrm{e}^{-\gamma t} + \vartheta_\infty \tag{19}$$

where $\gamma > 0$ is the index of rate of convergence, representing the lower bound of the rate of tracking error convergence. ϑ_1 and ϑ_∞ are reasonably selected positive real numbers. $e_1(0) < \vartheta_0$, $\vartheta_\infty < \vartheta_0$ is the steady-state error indicator.

Performance index $\vartheta(t)$ will converge exponentially to the final value ϑ_∞ in (19). Then, the boundary function is constructed from the performance indicator function to limit the tracking error of the system

$$\begin{cases} -R_L\vartheta(t) < e_1(t) < \vartheta(t), e_1(0) \geqslant 0 \\ -\vartheta(t) < e_1(t) < R_U\vartheta(t), e_1(0) \leqslant 0 \end{cases} \tag{20}$$

where $e_1(0)$ is the initial value of the tracking error $e_1(t)$, R_L and $R_U \in (0, 1]$ are constraints on the overshoot of the system response.

Next, normalizing Eq. (20) as follows

$$\begin{cases} -R_L < \frac{e_1(t)}{\vartheta(t)} < 1, e_1(0) \geqslant 0 \\ -1 < \frac{e_1(t)}{\vartheta(t)} < R_U, e_1(0) \leqslant 0 \end{cases} \tag{21}$$

Constructing a smooth and strictly monotonically increasing error transformation bijection $\Gamma(\cdot)$: $(-1, 1) \to (-\infty, \infty)$. This paper adopts the hyperbolic tangent form of the error conversion function

$$\Gamma(\varepsilon) = \begin{cases} \frac{\mathrm{e}^{\varepsilon} - \zeta\mathrm{e}^{-\varepsilon}}{\mathrm{e}^{\varepsilon} + \mathrm{e}^{-\varepsilon}}, \varepsilon \geqslant 0 \\ \frac{\zeta\mathrm{e}^{\varepsilon} - \mathrm{e}^{-\varepsilon}}{\mathrm{e}^{\varepsilon} + \mathrm{e}^{-\varepsilon}}, \varepsilon \leqslant 0 \end{cases} \tag{22}$$

According to $e_1(t) = \vartheta(t)\Gamma(\varepsilon)$ and the properties of hyperbolic tangent functions, the error conversion function can be transformed into

$$\varepsilon = \frac{1}{2}\ln\frac{1+\Gamma}{1-\Gamma} = \frac{1}{2}\ln\frac{1+\frac{e_1}{\vartheta}}{1-\frac{e_1}{\vartheta}} = \frac{1}{2}(\ln(\vartheta + e_1) - \ln(\vartheta - e_1)) \tag{23}$$

In order to facilitate the controller design later, some dynamic equations of the converted error function are calculated respectively as follows

$$\dot{\varepsilon} = \frac{1}{2}\left(\frac{\dot{\vartheta} + \dot{e}_1}{\vartheta + e_1} - \frac{\dot{\vartheta} - \dot{e}_1}{\vartheta - e_1}\right) \tag{24}$$

$$\begin{aligned} \ddot{\varepsilon} = {} & \frac{1}{2}\left(\frac{(\ddot{\vartheta} + \ddot{e}_1)(\vartheta + e_1) - (\dot{\vartheta} + \dot{e}_1)^2}{(\vartheta + e_1)^2} - \frac{(\ddot{\vartheta} - \ddot{e}_1)(\vartheta - e_1) - (\dot{\vartheta} - \dot{e}_1)^2}{(\vartheta - e_1)^2}\right) = \\ & \frac{\ddot{\vartheta}(\vartheta + e_1) - (\dot{\vartheta} + \dot{e}_1)^2}{2(\vartheta + e_1)^2} + \frac{\ddot{e}_1(\vartheta + e_1)}{2(\vartheta + e_1)^2} - \frac{\ddot{\vartheta}(\vartheta - e_1) - (\dot{\vartheta} - \dot{e}_1)^2}{2(\vartheta - e_1)^2} + \\ & \frac{\ddot{e}_1(\vartheta - e_1)}{2(\vartheta - e_1)^2} = \\ & \frac{\ddot{\vartheta}(\vartheta + e_1) - (\dot{\vartheta} + \dot{e}_1)^2}{2(\vartheta + e_1)^2} - \frac{\ddot{\vartheta}(\vartheta - e_1) - (\dot{\vartheta} - \dot{e}_1)^2}{2(\vartheta - e_1)^2} + \\ & \left(\frac{\vartheta + e_1}{2(\vartheta + e_1)^2} + \frac{\vartheta - e_1}{2(\vartheta - e_1)^2}\right)\ddot{e}_1 \end{aligned} \tag{25}$$

By deforming Eq. (25) for ease of calculation, it can be obtained that

$$\ddot{\varepsilon} = N + M\ddot{e}_1 \tag{26}$$

where $M = \frac{\vartheta + e_1}{2(\vartheta + e_1)^2} + \frac{\vartheta - e_1}{2(\vartheta - e_1)^2}$, $N = \frac{\ddot{\vartheta}(\vartheta + e_1) - (\dot{\vartheta} + \dot{e}_1)^2}{2(\vartheta + e_1)^2} - \frac{\ddot{\vartheta}(\vartheta - e_1) - (\dot{\vartheta} - \dot{e}_1)^2}{2(\vartheta - e_1)^2}$.

Remark 6. Obviously, $-R_L\vartheta(t)$ and $R_U\vartheta(t)$ limit the maximum overshoot of e_1 and the descent speed of $\vartheta(t)$ affects the convergence speed of e_1. $-\vartheta_\infty$ and ϑ_∞ determine the steady-state error range of e_1. Moreover, it can be verified that if ε converges, the error e_1 converges. And the range of values for ε is within the entire real space, then $\frac{e_1}{\vartheta}$ is bounded in $(-1, 1)$.

3.4. Composite controller design

The converted error can limit the dynamic performance of the system to a prescribed range. This section will design a new fixed-time controller based on prescribed performance which can improve the robustness of the system by compensating as well as suppressing output of RDO through feedforward.

The tracking error of the original system (6) is $e_1 = x_1 - x_r$ and first order and second order dynamics of e_1 are calculated as

$$\begin{cases} \dot{e}_1 = \dot{x}_1 - \dot{x}_r = x_2 + d_1 - \dot{x}_r \\ \ddot{e}_1 = \dot{x}_2 + \dot{d}_1 - \ddot{x}_r = g - Hu + d_2 + \dot{d}_1 - \ddot{x}_r \end{cases} \tag{27}$$

For the suspension system (6), use the transformed position error and velocity error to design the sliding surface

$$s(t) = \dot{\varepsilon} + \int_0^t \left(\lambda_1 \left| \varepsilon \right|^{\frac{m_1}{n_1}} \operatorname{sign}(\varepsilon(\mu)) + \beta_1 \left| \varepsilon \right|^{\frac{q_1}{p_1}} \operatorname{sign}(\varepsilon(\mu)) \right) \mathrm{d}\mu \tag{28}$$

where $\lambda_1 > 0$, $\beta_1 > 0$, $0 < m_1 < n_1$, $q_1 > p_1 > 0$.

Take the first derivative of the sliding surface

$$\dot{s} = \ddot{\varepsilon} + A_\varepsilon \tag{29}$$

where $A_\varepsilon = \lambda_1 |\varepsilon|^{\frac{m_1}{n_1}} \operatorname{sign}(\varepsilon) + \beta_1 |\varepsilon|^{\frac{q_1}{p_1}} \operatorname{sign}(\varepsilon)$.

Combining Eqs. (21) and (22) into Eq. (25), it can be obtained that

$$\begin{aligned} &\dot{s} = N + M\ddot{e}_1 + A_\varepsilon = \\ &M(g - Hu + d_2 + \dot{d}_1 - \ddot{x}_r) + N + A_\varepsilon \end{aligned} \tag{30}$$

To ensure that the sliding mode can keep on the sliding mode surface $s = 0$, a fixed-time controller is as follows

$$U = \frac{1}{H}(u_{eq} + u_{ob} + u_r) \tag{31}$$

in which the terms of u_{eq}, u_{ob} and u_r are designed as

$$\begin{cases} u_{eq} = g - \ddot{x}_r + M^{-1}N + M^{-1}A_\varepsilon \\ u_{ob} = \hat{d}_2 + \hat{\dot{d}}_1 \\ u_r = M^{-1}(\lambda_2 |s|^{\frac{m_2}{n_2}} \operatorname{sign}(s) + \beta_2 \left| s \right|^{\frac{q_2}{p_2}} \operatorname{sign}(s)) \end{cases} \tag{32}$$

where $\lambda_2 > 0$, $\beta_2 > 0$, $0 < m_2 < n_2$, $q_2 > p_2 > 0$.

3.5. Stability analysis

Theorem 1. For the suspension system presented in (6), if it chooses Eq. (28) as sliding mode surface and fixed-time control law is selected as Eq. (31), then the suspension system (6) is fixed-time stable. The steady-state performances of the suspension system such as overshoot and response time are guaranteed by prescribed tracking error performance.

PROOF OF THEOREM 1. Based on (30)–(32), the sliding mode state can be lead to

$$\dot{s} = -\lambda_2 \left| s \right|^{\frac{m_2}{n_2}} \operatorname{sign}(s) - \beta_2 \left| s \right|^{\frac{q_2}{p_2}} \operatorname{sign}(s) + \tilde{d}(t) \tag{33}$$

where $\tilde{d} = M((d_2 - \hat{d}_2) + (\dot{d}_1 - \hat{\dot{d}}_1))$ is system disturbance.

Next, we will analyze the stability of the sliding mode state under the assumption $|\tilde{d} \leqslant D|$ with a positive constant D.

The next step is a two-step stability proof.

Step 1: To prove that sliding mode state (28) is always in the following region

$$\Omega_s = \left\{ \varepsilon \in \mathbb{R} \left| |s| \leq \min \left(\frac{D}{\lambda_2} \right)^{\frac{n_2}{m_2}}, \left(\frac{D}{\beta_2} \right)^{\frac{p_2}{q_2}} \right. \right\} \tag{34}$$

Choose the Lyapunov function

$$V_1 = \frac{1}{2}s^2 \tag{35}$$

Based on (33), one can obtain

$$\begin{aligned} &\dot{V}_1 = s \cdot \dot{s} = s\left(-\lambda_2 \left| s \right|^{\frac{m_2}{n_2}} \operatorname{sign}(s) - \beta_2 \left| s \right|^{\frac{q_2}{p_2}} \operatorname{sign}(s) + \tilde{d}(t) \right) = - \\ &\lambda_2 \left| s \right|^{\frac{m_2}{n_2}+1} - \beta_2 \left| s \right|^{\frac{q_2}{p_2}+1} + s\tilde{d}(t) \leqslant \\ &-\lambda_2 \left| s \right|^{\frac{m_2}{n_2}+1} - \beta_2 \left| s \right|^{\frac{q_2}{p_2}+1} + D|s| \end{aligned} \tag{36}$$

Clearly, the equation contains positive sign terms. To ensure that all the right terms of the inequality are less than 0, change the inequality (36) into the following form

$$\dot{V}_1 \leqslant -\lambda_2 |s| \left(\left| s \right|^{\frac{m_2}{n_2}} - \frac{D}{\lambda_2} \right) - \beta_2 \left| s \right|^{\frac{q_2}{p_2}+1} \tag{37}$$

As long as the sliding mode state is ensured to satisfy $|s| \geqslant \left(\frac{D}{\lambda_2} \right)^{\frac{n_2}{m_2}}$, then

$$\dot{V}_1 \leqslant 0 \tag{38}$$

Using the same method, Eq. (30) can also be transformed into

$$\dot{V}_1 \leqslant -\beta_2 |s| \left(\left| s \right|^{\frac{q_2}{p_2}} - \frac{D}{\beta_2} \right) - \lambda_2 \left| s \right|^{\frac{m_2}{n_2}+1} \tag{39}$$

if the sliding mode state satisfy $|s| \geqslant \left(\frac{D}{\beta_2} \right)^{\frac{p_2}{q_2}}$, then $\dot{V}_1 \leqslant 0$.

Hence, the tracking error will gradually converge to the region Ω_s if the sliding mode state is selected as (28). Moreover, if the sliding surface is outside the region (34), then $\dot{V}_1 \leqslant 0$.

Step 2: To prove the sliding mode state (28) will converge to the region within a fixed-time.

Based on step 1, the next step is to prove that fixed time convergence does not consider disturbance $\tilde{d}(t)$ and Eq. (36) can be transformed into

$$\dot{V}_1 \leqslant -\lambda_2 \left| s \right|^{\frac{m_2}{n_2}+1} - \beta_2 \left| s \right|^{\frac{q_2}{p_2}+1} \tag{40}$$

Substituting $s = (2V)^{\frac{1}{2}}$ into (34) leads to

$$\dot{V}_1 \leqslant -\lambda_2 (2V_1)^{\frac{m_2+n_2}{2n_2}} - \beta_2 (2V_1)^{\frac{q_2+p_2}{2p_2}} \tag{41}$$

According to Definition 1 and Lemma 1, it can be calculated that the suspension system can converge the domain (34) no longer than a fixed-time t_s

$$t_s \leqslant t_{s_1} + t_{s_2} \tag{42}$$

where $t_{s_1} = 2^{-\frac{m_2-n_2}{2n_2}} \cdot \frac{n_2}{\lambda_2(n_2-m_2)}$, $t_{s_2} = 2^{-\frac{q_2-p_2}{2p_2}} \cdot \frac{p_2}{\beta_2(q_2-p_2)}$.

Therefore, the sliding mode can stably converge within a finite time. Finally, the position tracking error converges to the equilibrium point within a fixed-time and ensures the given control performance.

Asymptotically, this completes the proof.

4. Simulation results

In this section, there will be a simulation for the single electromagnet suspension system to verify the effectiveness of the control strategy in high-speed EMS trains with track irregularities. Some main system parameters considered are listed in Table 1. Then, some units are defined by x_1−cm, x_2−cm/s and $u - A^2$. The initial conditions of the suspension system are $x_1(0) = 12$ mm and $x_2(0) = 0$ cm/s. In reality, the standard of suspension air gap is around 8–12 mm. Therefore, the reference suspension air gap is selected as $x_r = 10$ mm in this paper.

The periodic track irregularity disturbance influenced by long waves is described to be $d_1 = f(\chi)\sin\left(\frac{2\pi v}{\chi}t\right)$, where χ and v are the wavelength of the irregularity and the velocity of the train, respectively. $f(\chi)$is the amplitude of the irregularity corresponding to χ [26]. The disturbance d_1 can be modeled as (8), where the coefficient matrices are

$$\boldsymbol{W} = \begin{bmatrix} 0 & \frac{2\pi v}{\chi} \\ -\frac{2\pi v}{\chi} & 0 \end{bmatrix} \quad V = [1 \quad 0] \tag{43}$$

Simulating the actual maglev train operation and setting the speed v to 430 km/h and the parameters χ is chosen as 475 m.

In addition, d_2 containing uncertainty Δh and exogenous disturbance F_e which are selected as 0.1h and $\sin(2.52\pi t) + \sin(0.2\pi t)$.

For obtaining satisfactory control results, the controller parameters are presented in Table 2. The following contents are the details of the simulation results.

Fig. 3 and Fig. 4 respectively show actual track irregularities disturbance d_1 and the lumped disturbances d_2 with uncertainty and exogenous disturbances, as well as the estimation of two types of disturbances (the output of RDO) and the estimation error. It can be seen

Table 1
Main parameters of suspension system.

System parameter	Value	Unit
g	980	cm/s^2
m	0.75	ton
μ_0	$4\pi \times 10^{-7}$	NA^{-2}
S	230	cm^2
N	300	

Table 2
Controller parameters of the proposed strategy.

Parameter	Value	Parameter	Value	Parameter	Value
L	$[100 \quad 100]^T$	λ_1	5000	λ_2	40
η_1	400	β_1	5000	β_2	40
η_2	4×100^4	m_1	9	m_2	9
ϑ_0	4	n_1	10	n_2	10
ϑ_∞	1	q_1	0.111	q_2	0.111
γ	2	p_1	0.1	p_2	0.1

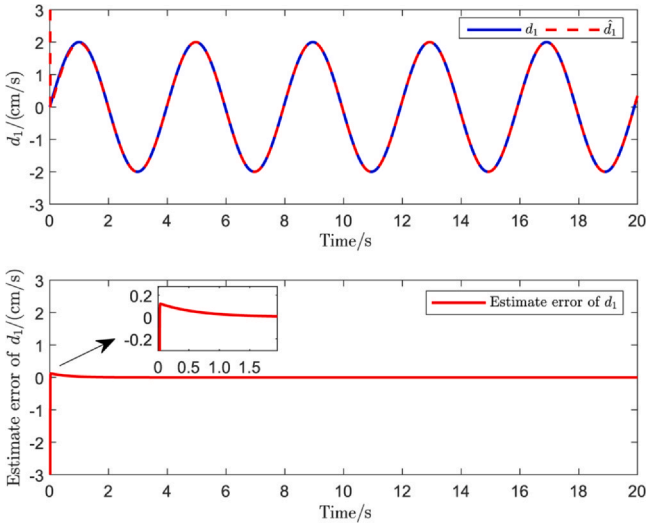

Fig. 3. The performance of RDO in estimating d_1 and the estimate error of d_1.

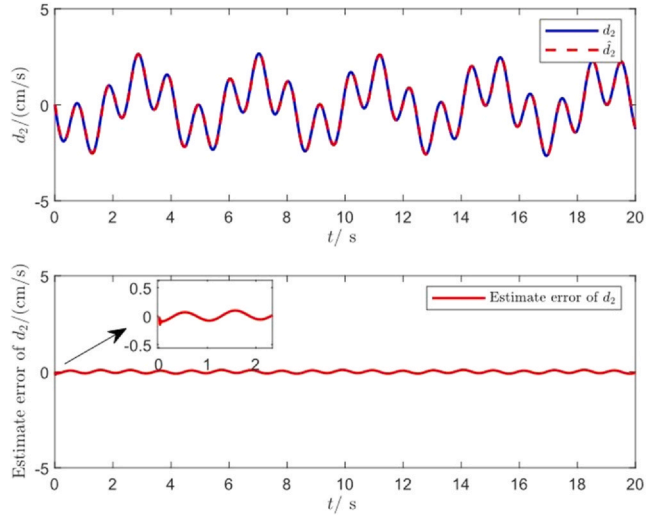

Fig. 4. The performance of RDO in estimating d_2 and the estimating error of d_2.

that the designed RDO can accurately estimate disturbances and has satisfactory estimation performance. Hence, these two figures demonstrate the effectiveness of RDO in disturbance estimation.

Through the proposed RDO-PPFTC strategy, the suspension air gap and vertical velocity trajectory response of the suspension system are displayed in Fig. 5. From it, it can be seen that under the RDO-PPFTC algorithm, the suspension air gap x_1 can converge to the expected fixed value in about 0.2 s. The system has fast response speed and good stability performance. Similarly, the vertical speed x_2 also converges to the reference value around 0.2 s, ensuring that the train can run smoothly even under high-speed conditions, even under irregular tracks and external disturbances.

Fig. 6 shows the tracking error of the suspension air gap x_1 and the prescribed-performance function $\vartheta(t)$. From the Fig. 6, it can be seen that the preset performance function $\vartheta(t)$ has a good effect of limiting the upper and lower bounds of tracking error. In order to convert tracking errors from a constrained space to an unconstrained space effectively, the algorithm should be utilized.

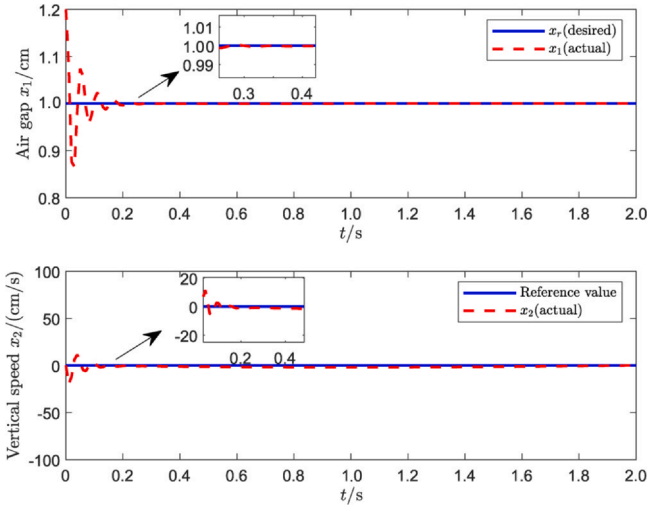

Fig. 5. The trajectory response of suspension air gap x_1 and vertical velocity x_2.

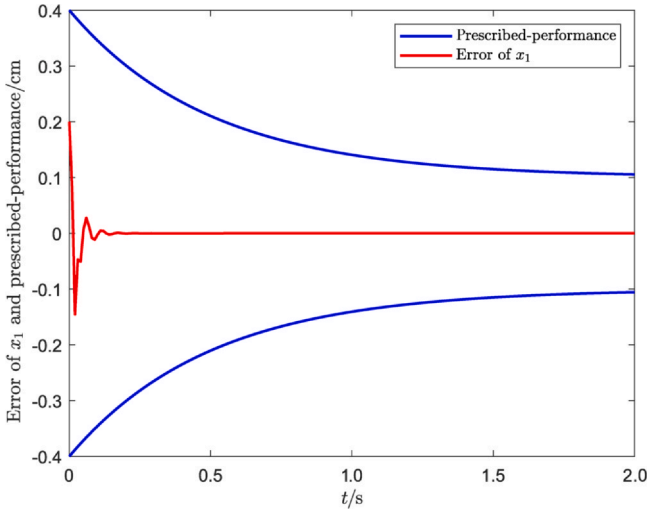

Fig. 6. The response of tracking error of suspension air gap x_1 and prescribed-performance function $\vartheta(t)$.

5. Conclusion

In this paper, a fixed-time controller with prescribed-performance based on refined disturbance observer is proposed to handle the fast dynamics and rapid change of irregularities problem of the high-speed electromagnetic suspension train under the continuous excitation of track irregularities at high speed. The refined disturbance observer can accurately estimate track irregularities and lumped disturbances with uncertainties and exogenous disturbances, and the fixed-time controller based on prescribed performance can quickly compensate for disturbances within a fixed time. The simulation results on the suspension system indicate that proposed control scheme improves the suspension air gap response and enhances the stability of train operation. In the future, the impact of high-speed compressed air flow between the vehicle body and track on the suspension system can be considered, and the control algorithm can be extended to the semi bogies or full bogies of the trains and verified on the testing lines.

Acknowledgments

This work was supported by the National Natural Science Foundation of China (Grant 62273029).

References

[1] H. Lee, K. Kim, J. Lee, Review of maglev train technologies, IEEE Trans. Magn. 42 (2006) 1917–1925.
[2] G. Marjan, T. Boris, Modeling and control of the magnetic suspension system, ISA Trans. 42 (2003) 89–100.
[3] J. Wang, J. Rong, J. Yang, Adaptive fixed-time position precision control for magnetic levitation systems, IEEE Trans. Autom. Sci. Eng. 20 (2022) 458–469.
[4] J. Wang, L. Zhao, L. Yu, Adaptive terminal sliding mode control for magnetic levitation systems with enhanced disturbance compensation, IEEE Trans. Ind. Electron. 68 (2020) 756–766.
[5] J. Shi, W. Fang, Y. Wang, et al., Measurements and analysis of track irregularities on high-speed maglev lines, J. Zhejiang Univ. Sci. A 15 (2014) 385–394.
[6] P. Yu, J. Li, L. Wang, Influence of track periodical irregularities to the suspension system of low-speed maglev vehicle, in: Proceedings of the 2015 34th Chinese Control Conference (CCC), (2015)8479–8484.
[7] T. Albert, G. Oleszczuk, On the influence of structural flexibility on feedback control system stability for ems maglev vehicles, J. Dyn. Syst. Meas. Control Trans. ASME 133 (2011) 1–6.
[8] J. Li, D. Zhou, P. Yu, Self-excited vibration problems of maglev vehicle-bridge interaction system, J. Cent. South Univ. 21 (2014) 4184–4192.
[9] X. Lei, H. Wang, Dynamic analysis of the high-speed train-track spatial nonlinear coupling system under track irregularity excitation, Int. J. Struct. Stab. Dyn. 23 (14) (2023).
[10] F. El-Sousy, K. Alattas, O. Mofid, et al., Non-singular finite time tracking control approach based on disturbance observers for perturbed quadrotor unmanned aerial vehicles, Sensors 22 (2022) 2785.
[11] T. Truong, A. Vo, H. Kang, A backstepping global fast terminal sliding mode control for trajectory tracking control of industrial robotic manipulators, IEEE Access 9 (2021) 31921–31931.
[12] A. Levant, Chattering analysis, IEEE Trans. Autom. 55 (2010) 1380–1389.
[13] L. Fridman, et al., J. Moreno, B. Bandyopadhyay, Continuous nested algorithms: the fifth generation of sliding mode controllers, Recent Advances in Sliding Modes: From Control to Intelligent, Mechatronics (2015) 5–35.
[14] C. Mu, H. He, Dynamic behavior of terminal sliding mode control, IEEE Trans. Ind. Electron. 65 (2017) 3480–3490.
[15] H. Pan, G. Zhang, H. Ouyang, et al., A novel global fast terminal sliding mode control scheme for second-order systems, IEEE Access 8 (2020) 22758–22769.
[16] Y. Feng, X. Yu, F. Han, On nonsingular terminal sliding-mode control of nonlinear systems, Automatica 49 (2013) 1715–1722.
[17] S. Lian, W. Meng, Z. Lin, et al., Adaptive attitude control of a quadrotor using fast nonsingular terminal sliding mode, IEEE Trans. Ind. Electron. 69 (2022) 1597–1607.
[18] J. Yang, A. Zolotas, W. Chen, et al., Robust control of nonlinear MAGLEV suspension system with mismatched uncertainties via DOBC approach, ISA Trans 50 (2011) 389–396.
[19] J. Han, From PID to active disturbance rejection control, IEEE Trans. Ind. Electron. 56 (2009) 900–906.
[20] L. Guo, W. Chen, Disturbance attenuation and rejection for systems with nonlinearity via dobc approach, Int. J. Robust Nonlinear Control 15 (2005) 109–125.
[21] X. Yao, L. Zhang, W. Zheng, Uncertain disturbance rejection and attenuation for semi-markov jump systems with application to 2-degree-freedom robot arm, IEEE Trans. Circuits Syst. I-Regul. Pap. 68 (2021) 3836–3845.
[22] X. Yao, J. Park, L. Wu, et al., Disturbance-observer-based composite hierarchical anti-disturbance control for singular markovian jump systems, IEEE Trans. Autom. Control 64 (2019) 2875–2882.
[23] X. Yao, L. Wu, L. Guo, Disturbance-observer-based fault tolerant control of high-speed trains: a markovian jump system model approach, IEEE Trans. Syst. Man Cybern. Syst. 50 (2019) 1476–1485.
[24] T. Truong, A. Vo, H. Kang, et al., An observer-based fixed time sliding mode controller for a class of second-order nonlinear systems and its application to robot manipulators, Proc. Int. Conf. Intell. Comput. (2022) 529–543.
[25] J. Huang, M. Zhang, S. Ri, et al., High-order disturbance-observer-based sliding mode control for mobile wheeled inverted pendulum systems, IEEE Trans. Ind. Electron. 67 (2019) 2030–2041.
[26] S. Jiang, D. Shen, T. Zhang, et al., Nonlinear robust composite levitation control for high-speed ems trains with input saturation and track irregularities, IEEE Trans. Intell. Transp. Syst. 23 (2022) 20323–20336.
[27] S. Jiang, H. Xu, T. Zhang, et al., Lazy prescribed-time synchronization control of half bogiefor high-speed maglev train considering track irregularities and input constraints, IEEE Trans. Veh. Technol. 71 (2022) 6924–6937.
[28] J. Wang, L. Zhao, L. Yu, Adaptive terminal sliding mode control for magnetic levitation systems with enhanced disturbance compensation, IEEE Trans. Ind. Electron. 68 (2021) 756–766.
[29] N. Boonsatit, N. Pukdeboon, Adaptive fast terminal sliding mode control of magnetic levitation system, J. Control Autom. Electr. Syst. 27 (2016) 359–367.
[30] A. Sharma, A. Alturki, S. Amrr, Extended state observer based integral sliding mode control for maglev system with fixed time convergence, IEEE Access 10 (2022) 93074–93083.

[31] P. Chen, T. Shi, M. Yu, et al., Sliding mode active disturbance rejection levitation control algorithm of the medium- and low-speed maglev vehicles, J. Railw. Sci. Eng. 20 (2023) 682–693.
[32] A. Polyakov, Nonlinear feedback design for fixed-time stabilization of linear control systems, IEEE Trans. Autom. Control 57 (2012) 2106–2110.
[33] Z. Zuo, Non-singular fixed-time terminal sliding mode control of nonlinear systems, IET Control Theory Appl. 9 (2015) 545–552.
[34] Z. Gao, Scaling and bandwidth-parameterization based controller tuning, in: Proceedings of the 2003 American Control Conference (2005) 4989-4996.
[35] L. Guo, Y. Zhu, W. Li, An enhanced anti-disturbance control approach for systems subject to multiple disturbances, 2018 Chinese Automation Congress (CAC) (2018) 2785-2790.